brief communication

Intracellular magnesium blocks sodium outward currents in a voltage- and dose-dependent manner

Michael Pusch,* Franco Conti,‡ and Walter Stühmer*
*Max-Planck-Institut für biophysikalische Chemie, D-3400 Göttingen, Federal Republic of Germany; and ‡Istituto di Cibernetica e Biofisica, I-16146 Genova, Italy

ABSTRACT Tail currents through Na^+ channels have been measured in inside-out patches from *Xenopus laevis* oocytes injected with cDNA-derived mRNA coding for the rat brain type II Na^+ channel. It is shown that intracellular Mg^{2+} blocks outward currents in a voltage- and dose-dependent manner with a half blocking concentration between 3 and 4 mM at 0 mV and a voltage dependence of *e*-fold per 49 mV.

INTRODUCTION

In several preparations where outward Na^+ currents have been studied, a decrease of the maximum conductance has been observed at large depolarizations (e.g., rat muscle, Pappone [1980]; human and rat skeletal muscle, Almers et al. [1984]; frog oocytes with injected Na^+ channel mRNA, Stühmer et al. [1987]). Because the Hodgkin-Huxley model of the Na^+ permeability combined with the Goldman-Hodgkin-Katz current equation predicts a constant value of the conductance at high potentials, the observed decrease of the conductance has been attributed mainly to the nonvalidity of the constant field equation at high membrane potentials.

We have investigated Na^+ outward currents in inside-out patches, which allow control of the intracellular ion composition, and find that the decrease of the Na^+ channel conductance at high potentials can be explained by a blocking action of intracellular Mg^{2+} in a voltage- and dose-dependent manner. The block by Mg^{2+} shows a half blocking concentration between 3 and 4 mM at 0 mV and a voltage dependence of *e*-fold per 49 mV.

Similar inhibitory effects of intracellular Mg^{2+} have been reported for outward currents through several channels (e.g., ATP-sensitive K^+ channels [Horie et al., 1987], inwardly rectifying K^+ channels [Matsuda, 1988], Ca^{2+} channels [White and Hartzell 1988], muscarinic K^+ channels [Horie and Irisawa 1987]). Also inward currents, especially through *N*-methyl-D-aspartate (NMDA)-activated channels (Mayer et al., 1984) can be blocked by Mg^{2+}. We propose that the reduction in sodium conductance for outward currents is caused by intracellular Mg^{2+} block.

METHODS

Experimental conditions

Sodium currents were recorded from inside-out patches from *Xenopus laevis* oocytes injected with cDNA derived mRNA coding for the type II rat brain sodium channel (Noda et al., 1986) using standard patch clamp techniques (Hamill et al., 1981).

The procedures of oocyte injection and preparation are described elsewhere (Methfessel et al., 1986; Stühmer et al., 1987). The inside-out patches were obtained by withdrawal of the patch pipette after obtaining a "gigaseal." This often resulted in formation of vesicles at the tip of the pipette as witnessed by distorted current kinetics and small current amplitudes resulting from poor voltage control. Vesicles could not be opened by short air exposure of the pipette (Hamill et al., 1981) because this resulted in most cases in the destruction of the patch. However, we found that gently touching a Sylgard ball attached to a nearby pipette often yielded proper inside-out patches with the intracellular side of the membrane exposed to the bath, as judged from the expected behavior of the Na^+ currents. Patch pipettes had resistances between 1 and 2 MΩ. Due to the high density of sodium channels expressed in oocytes after injection of type II rat brain sodium channel mRNA, patches formed with large tip electrodes usually contain a large number of channels (Stühmer et al., 1987).

The pipette solution contained (in millimolar): 115 NaCl, 2.5 KCl, 1.8 $CaCl_2$, 10 Hepes-NaOH, pH 7.2. The bath solution contained 90 KCl, 30 NaCl, 10 NaOH-EGTA, 10 Hepes-KOH, pH 7.2, and different amounts of $MgCl_2$ (0, 0.5, 1, 2, 3, 4, and 5 mM). The experiments shown in Fig. 1 were done with a different bath solution: 110 KCl, 10 EGTA-NaOH, 10 Hepes-KOH, pH 7.2. All experiments were performed at 15–16°C.

Current recording and stimulation was controlled by a DEC-PDP-11/73 laboratory computer. Currents were filtered by an eight-pole Bessel filter with a cut-off frequency of 10 kHz. "Tail" currents were measured using the following pulse protocol. From the holding potential (−90 to −120 mV) a short (0.3–0.5 ms) depolarizing voltage step to 30 mV which activated the channels without appreciable inactivation was followed by a test pulse to various test potentials (from −60 mV to +120 mV in 10-mV steps) which elicited a declining tail current (see Fig. 2). Linear leakage and capacitive currents were subtracted on-line using a P/4-method (Bezanilla and Armstrong, 1977).

Analysis

Tail currents were analyzed by fitting an exponential function to the first part of the tail current, excluding the rise time at the beginning of the tail current, and extrapolating this exponential function to the time of the onset of the test pulse. The extrapolated current values were then used to construct "instantaneous" current voltage relationships (Fig. 3). These reflect the permeability properties of the channel without interference from the kinetic properties because at the onset of the tail pulse

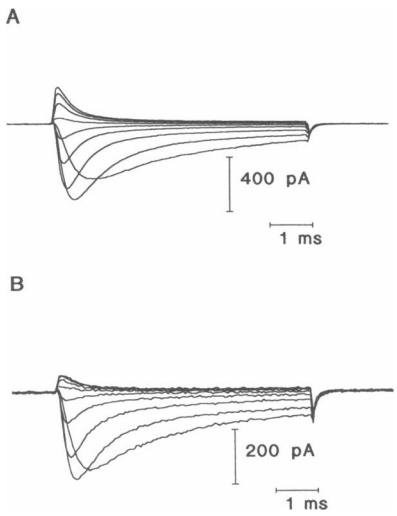

FIGURE 1 Families of currents elicited in an inside-out patch by voltage steps from a holding potential of −100 mV to various test potentials from −30 to 130 mV in 20-mV steps. Each trace is the average of 16 records after subtraction of linear leak and capacitive currents. Solutions are as described in Methods with (*A*) 1 mM Mg^{2+} and (*B*) 5 mM Mg^{2+}. The currents are from the same patch. Currents in *B* were obtained after perfusing the bath for ~2 min with the 5 mM Mg^{2+} solution.

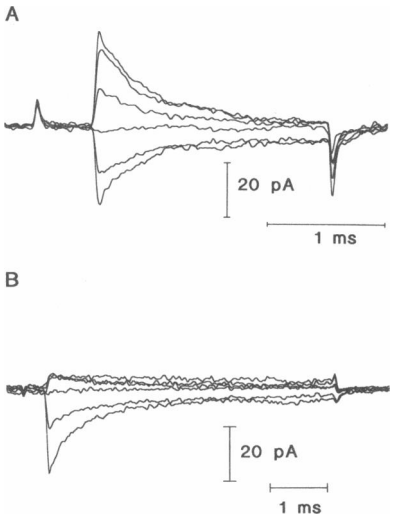

FIGURE 2 Tail currents from two different patches. After a prepulse to 30 mV the potential was stepped to −30, 0, 30, 60, 90, and 120 mV giving rise to the tail currents shown. Each trace is the average of eight records. Solutions are as described in Methods with (*A*) 0 mM Mg^{2+} and (*B*) 5 mM Mg^{2+}. The prepulse is hardly visible in the figure since the prepulse potential (30 mV) is near the reversal potential so that even though the channels are activated little current flows through them.

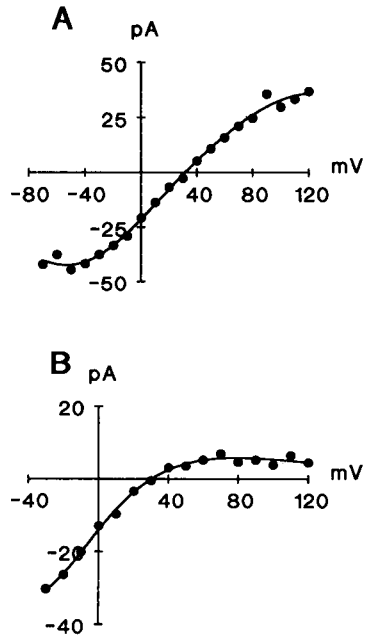

FIGURE 3 Instantanous current voltage relationships derived from the currents shown in Fig. 2. (In Fig. 2 not all current traces are shown for clarity.) (*A*) 0 mM Mg^{2+}; (*B*) 5 mM Mg^{2+}. Symbols represent the extrapolated current amplitudes at the onset of the tail pulse. Solid lines represent fits of Eq. 4 to the data points. The parameters obtained are (*A*) E_{rev} = 31.3 mV, $P = 1.04 \cdot 10^{-16}$ mol s^{-1}, A = 0.197, B = 33.2 mV, C = 0.0054, and V_H = 29.5 mV, and (*B*) E_{rev} = 30.3 mV, $P = 2.20 \cdot 10^{-16}$ mol s^{-1}, A = 0.184, B = 22.0 mV, C = 2.015, and V_H = 51.4 mV.

the degree of activation and inactivation of the channels in the patch is the same for all tail potentials.

All fitting procedures were based on the least squares method.

RESULTS

The qualitative effect of intracellular Mg^{2+} is illustrated in Figs. 1 and 2. Fig. 1 shows families of current traces elicited by voltage steps from −100 mV to various test potentials at 1 mM Mg^{2+} (Fig. 1 *A*) and 5 mM Mg^{2+} (Fig. 1 *B*) from the same patch. It can be seen that the overall current magnitude is smaller at the higher Mg^{2+} concentration (note the change in scale) and that the kinetics of the currents are slightly different. The lower current amplitude in Fig. 1 *B* compared with Fig. 1 *A* is possibly due to a "rundown" of Na^+ channels during the perfusion. Because we could not routinely change the bath solution during an experiment (the patch often broke during the perfusion) we concentrated on the reduction of the outward currents as compared with the magnitude of the inward currents, as illustrated in Fig. 1, and which can

be studied without perfusing the same patch with different bath solutions.

Fig. 2 shows tail currents from two different patches at 0 and 5 mM Mg^{2+}, respectively, with higher Na^+ concentrations in the bath than in Fig. 1 (30 mM) to increase the magnitude of the outward currents. The reduction of the outward currents compared with the inward currents is obvious. The overall current magnitude in Fig. 2 is lower than in Fig. 1 because the experiments were performed with different oocytes with a lower level of expression and because in Fig. 2 smaller patch pipettes were used.

For a quantitative description of the Mg^{2+} block we assumed that the probability of the channel being blocked is given by a Boltzmann factor,

$$p = \frac{1}{1 + C\exp\left(\frac{V}{V_H}\right)}, \quad (1)$$

where V is the membrane potential, V_H represents the steepness of the voltage dependence, and C determines the absolute magnitude of the block at a given potential. A linear relationship between C and the intracellular Mg^{2+} concentration would be expected for a simple blocking reaction. It can be seen in Fig. 3 *A* that there is also a flattening of inward currents at low potentials. This could be due to a blocking action of extracellular Ca^{2+} (Taylor et al., 1976; Nilius, 1988; Tanguy and Yeh, 1988). To account for this upward deflection we included a factor similar to Eq. 1 in the description:

$$q = \frac{1}{1 + A\exp\left(\frac{-V}{B}\right)}, \quad (2)$$

without attempting to interpret the meaning of the parameters A and B. This factor has an influence on the current amplitude only at negative potentials and is merely included to fit the "instantaneous" current voltage relationships at negative potentials.

In the absence of intracellular and extracellular blocking agents we assumed that the current is given by the Goldman-Hodgkin-Katz current equation

$$I = P\frac{VF^2}{RT}\frac{1 - \exp\left(\frac{-(V - E_{rev})F}{RT}\right)}{1 - \exp\left(\frac{-VF}{RT}\right)}, \quad (3)$$

where E_{rev} is the reversal potential and the remaining symbols have their usual meaning. Within the model a complete description of the peak tail current is given by a combination of Eqs. 1–3.

$$I = P\frac{VF^2}{RT}\frac{1 - \exp\left(\frac{-(V - E_{rev})F}{RT}\right)}{1 - \exp\left(\frac{-VF}{RT}\right)}\frac{1}{1 + A\exp\left(\frac{-V}{B}\right)} \cdot \frac{1}{1 + C\exp\left(\frac{V}{V_H}\right)}. \quad (4)$$

Fig. 3. shows instantaneous current voltage relationships derived from the tail currents shown in Fig. 2. The solid lines represent least squares fits of Eq. 4 to the data points with P, E_{rev}, A, B, C, and V_H as free parameters. As mentioned above, the parameters A and B do not significantly interfere with the relevant parameters C and V_H which are mainly fixed by the data points at positive potentials. The reversal potential E_{rev} is a priori limited to a narrow voltage interval and it is not essential that it is included in the fit as a free parameter. It can be seen that the I-V curves can be well described by Eq. 4. Especially the sublinear behavior at high potentials and high Mg^{2+} concentrations can be described by a factor of the form given in Eq. 1.

Table 1 lists the values of the equilibrium potential V_H obtained from the fits of several experiments. No significant correlation with the Mg^{2+} concentration can be observed (linear correlation coefficient, 0.4). The mean value (±SD) for V_H is 49 ± 13 mV.

The concentration dependence of the block is illustrated in Fig. 4, where the parameter C (c.f. Eq. 4) is plotted versus the Mg^{2+} concentration. Obviously C increases with increasing Mg^{2+} concentration. However there seems to be a supralinear relation between C and the Mg^{2+} concentration. Half blocking of intracellular Mg^{2+} at 0 mV occurs at $C = 1$ according to Eq. 1. From Fig. 4 it can be seen that C is of the order of 1 at Mg^{2+} concentrations between 3 and 4 mM Mg^{2+}.

TABLE 1 Fitted values for the equilibrium potential V_H (see Eq. 4) at different Mg^{2+} concentrations

Mg^{2+}	V_H
mM	*mV*
0	39 (n = 3)
0.5	40 (n = 1)
1	42 (n = 2)
2	32 (n = 2)
3	51 (n = 3)
4	60 (n = 5)
5	56 (n = 2)

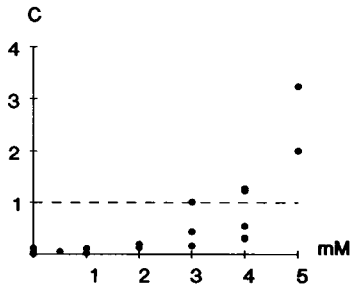

FIGURE 4 The parameter C (Eq. 4) obtained from several experiments is plotted versus the Mg^{2+} concentration. Horizontal dashed line shows that $C \approx 1$ between 3 and 4 mM.

DISCUSSION

Although much electrophysiological work has been done on the voltage-activated Na^+ channel, outward currents have often been neglected. Sublinear voltage dependence of outward currents at high potentials, resulting in a reduction of conductance above the reversal potential, which deviates from the prediction of the Goldman-Hodgkin-Katz current equation, have mostly been attributed to the nonvalidity of the GHK equation at high potentials. The GHK current equation is based on the assumption of a constant electric field along the permeation pathway and on the independence principle, which states that ion permeation is independent of the presence or concentration of other ions. Several studies have shown that these assumptions do not hold for the Na^+ channel (e.g., Begenisch and Cahalan, 1980*a*, and *b*). Nevertheless the GHK current equation adequately describes voltage and concentration dependence of Na^+ permeability, at least for moderate concentrations of permeable ions. For example Begenisch and Cahalan (1980*b*) report a half saturation internal Na^+ activity of 640 mM at 75 mV in internally perfused squid axons, which is much higher than the concentrations used here.

The data presented here show that deviations from the GHK current equation at high membrane depolarizations but physiological Na^+ concentrations can be accounted for by a voltage- and dose-dependent blocking action of intracellular Mg^{2+} ions.

Half blocking at 0 mV occurs at Mg^{2+} concentrations of $\approx$4 mM. This value can be compared with physiological intracellular Mg^{2+} concentrations. Unfortunately only few measurements of free intracellular Mg^{2+} concentrations exist. Alvarez-Leefmans et al. (1986) report a value of (1.69 ± 0.21) mM of free Mg^{2+} in frog skeletal muscle, which is probably of the same order of magnitude in most cells.

Screening of negative surface charges at the intracellular side of the membrane could be proposed as an alternative mechanism for the blocking effect of Mg^{2+}. We have not rigorously ruled out this possibility by testing other divalent or monovalent cations as blocking agents. However the quite low half blocking concentration of $\approx$4 mM found here, compared for example with 35 mM external Mg^{2+} needed to reduce the inward single channel conductance of heart Na^+ channels from 26 to 20 pS (Nilius, 1988), makes the mechanism of surface charge screening unlikely.

It will be interesting to study the blocking effect of Mg^{2+} at the single channel level. However measurement of outward single unmodified Na^+ channel currents presents special experimental difficulties due to large capacitive transients after stepping the membrane potential from the holding potential to, for example, 100 mV and to the short open time of the channels which mostly open soon after the voltage step.

There might be other effects of intracellular Mg^{2+} on the sodium channel. For example, we cannot rule out the possibility that Mg^{2+} also causes a reduction of inward currents in high intracellular Mg^{2+} (see Fig. 1). However we could not study these effects in detail since the "macropatches" were not stable enough to survive changes in solution. Because the level of expression and the patch size are so variable we limited our study to the intracellular block of Na^+ channels by Mg^{2+} and from our experiments it is clear that at physiological levels of Mg^{2+} a significant reduction of outward currents can be observed.

This block seems to be quite a general feature of ion channels. Intracellular Mg^{2+} reduces single channel currents through ATP-sensitive potassium channels in guinea-pig ventricular cells. Horie et al. (1987) report a K_D of 2.0 mM at 0 mV assuming a Hill coefficient of 1. This value is comparable with the 3–4 mM obtained here although our data cannot be described by a Hill coefficient of 1. Also Ca^{2+} currents in frog cardiac myocytes (White and Hartzell, 1988) and muscarinic K^+ currents in guinea pig atrial cells (Horie and Irisawa, 1987) are reduced by intracellular Mg^{2+} within this concentration range. Inwardly rectifying potassium channels in guinea pig heart cells are blocked by intracellular Mg^{2+} with a half-blocking concentration of 1.7 μM at 70 mV (Matsuda, 1988). This is far below the concentrations used here and argues against a common blocking mechanism in Na^+ channels and inwardly rectifying potassium channels.

The supralinear dependence on the Mg^{2+} concentration of the reduction of current indicates that more than one site of action is involved. From the voltage dependence a simple block might be a possible explanation, but not

consistent with the mentioned nonlinearity. This suggests a mechanism more complicated than simple block. Further studies are needed to resolve this question.

We thank Dr. H. Suzuki for help with the injection of oocytes, Drs. R. Penner, F. J. Sigworth, and M. B. Jackson for critical comments on the manuscript, and Prof. S. Numa, Dr. M. Noda, and their collaborators in Kyoto for supplying us with mRNA.

Received for publication 31 August 1988 and in final form 13 January 1989.

REFERENCES

Almers, W., W. M. Roberts, and R. L. Ruff. 1984. Voltage clamp of rat and human skeletal muscle: measurements with an improved loose-patch technique. *J. Physiol.* (*Lond.*). 347:751–768.

Alvarez-Leefmans, F. J., S. M. Gamino, F. Giraldez, and H. Gonzales-Serratos. 1986. Intracellular free magnesium in frog skeletal muscle fibres measured with ion-selective micro-electrodes. *J. Physiol.* (*Lond.*). 378:461–483.

Begenisch, T. B., and M. D. Cahalan. 1980*a*. Sodium channel permeation in squid axons. I. Reversal potential measurements. *J. Physiol.* (*Lond.*) 307:217–242.

Begenisch, T. B., and M. D. Cahalan. 1980*b*. Sodium channel permeation in squid axons. II. Non-independence and current-voltage relations. *J. Physiol.* (*Lond.*) 307:243–257.

Bezanilla, F., and M. Armstrong. 1977. Inactivation of the sodium channel. *J. Gen. Physiol.* 70:549–566.

Hamill, O. P., A. Marty, E. Neher, B. Sakmann, and F. J. Sigworth. 1981. Improved patch-clamp techniques for high-resolution current recording from cells and cell-free membrane patches. *Pfluegers Arch. Eur. J. Physiol.* 391:85–100.

Horie, M., and H. Irisawa. 1987. Rectification of muscarinic K^+ current by magnesium ion in guinea pig atrial cells. *Am. J. Physiol.* 253:H210–H214.

Horie, M., H. Irisawa, and A. Noma. 1987. Voltage-dependent magnesium block of adenosine-triphosphate-sensitive potassium channel in guinea-pig ventricular cells. *J. Physiol.* (*Lond.*) 387:251–272.

Matsuda, H. 1988. Open-state substructure of inwardly rectifying potassium channels revealed by magnesium block in guinea-pig heart cells. *J. Physiol.* (*Lond.*). 397:237–258.

Mayer, M. L., G. L. Westbrook, and P. B. Guthrie. 1984. Voltage-dependent block by Mg^{2+} of NMDA responses in spinal cord neurones. *Nature* (*Lond.*). 309:261–263.

Methfessel, C., V. Witzemann, T. Takahashi, M. Mishina, S. Numa, and B. Sakmann. 1986. Patch clamp measurements on Xenopus laevis oocytes: currents through endogenous channels and implanted acetylcholine receptor and sodium channels. *Pfluegers Arch. Eur. J. Physiol.* 407:577–588.

Nilius, B. 1988. Calcium block of guinea-pig heart sodium channels with and without modification by the piperazinylindole DPI 201-106. *J. Physiol.* (*Lond.*). 399:537–558.

Noda, M., T. Ikeda, T. Kayano, H. Suzuki, H. Takeshima, M. Kurasaki, H. Takahashi, and S. Numa. 1986. Existence of distinct sodium channel messenger RNAs in rat brain. *Nature* (*Lond.*). 320:188–192.

Pappone, P. A. 1980. Voltage-clamp experiments in normal and denervated mammalian skeletal muscle fibres. *J. Physiol.* (*Lond.*). 306:377–410.

Stühmer, W., C. Methfessel, B. Sakmann, M. Noda, and S. Numa. 1987. Patch clamp characterization of sodium channels expressed from rat brain cDNA. *Eur. Biophys. J.* 14:131–138.

Tanguy, J., and J. Z. Yeh. 1988. Divalent cation block of normal and BTX-modified sodium channels in squid axons. *Biophys. J.* 53:229a.

Taylor, R. E., C. M. Armstrong, and F. Bezanilla. 1976. Block of sodium channels by external calcium ions. *Biophys. J.* 16:27a.

White, R., and H. C. Hartzell. 1988. Effects of intracellular free magnesium on calcium current in isolated cardiac myocytes. *Science* (*Wash. DC*). 239:778–780.